Epileptiform activity generation by an ensemble of complete electronic FitzHugh-Nagumo oscillators connected by a sigmoid couplings

Egorov, Nikita, Sysoev, Ilya, Ponomarenko, Vladimir, Sysoeva, Marina

Nikita M. Egorov, Ilya V. Sysoev, Vladimir I. Ponomarenko, Marina V. Sysoeva, "Epileptiform activity generation by an ensemble of complete electronic FitzHugh-Nagumo oscillators connected by a sigmoid couplings," Proc. SPIE 12194, Computational Biophysics and Nanobiophotonics, 1219403 (29 April 2022); doi: 10.1117/12.2623993

SPIE.

Event: XXV Annual Conference Saratov Fall Meeting 2021; and IX Symposium on Optics and Biophotonics, 2021, Saratov, Russian Federation

Epileptiform activity generation by an ensemble of complete electronic FitzHugh-Nagumo oscillators connected by a sigmoid couplings

Nikita M. Egorov[a], Ilya V. Sysoev[b], Vladimir I. Ponomarenko[c], Marina V. Sysoeva[a]

[a]Yuri Gagarin State Technical University of Saratov, Saratov, Russia;
[b]Saratov State University, Saratov, Russia;
[c]Saratov Branch of the Institute of Radioengineering and Electronics of Russian Academy of Sciences, Saratov, Russia.

ABSTRACT

This work aims to show that the radioengineering generators able to demonstrate neural like activity can switch to the epileptiform behavior due to short time external driving if coupled using sigmoid function. The effect takes place for various number of generators in ensemble. The particular coupling architecture and initial phase of external driving are of importance.

Keywords: FitzHugh–Nagumo electronic generator, sigmoid coupling, thalamocortical brain network, epileptiform activity

1. INTRODUCTION

Recently,[1] the radioengineering realization of mesoscale hierarchically organized neural network model of brain thalamocortical system was proposed. This network was proved to generate epileptiform activity in response to external input in the form of a small sequence of pulses, which is a valid scenario of seizure initiation as shown for both humans and rats.[2] In this scenario an external input from peripheral nervous system (e. g. from nervus trigeminus) excites the thalamus and provokes a seizure.

This network model can be downscaled to some minimal number of elements, for which the desired regimes are kept. Since the connectivity matrix of the model has to be anatomically relevant and arbitrary couplings are not possible, this minimal number is not very small. In particular, in[1,3] the networks of 14 elements were considered and this number cannot be reduced significantly. Even for 14-element matrices the quantitative representation of experimental phenomena occurred to be not possible and only qualitative match was achieved. By the opposite, an increase of number of elements in the network should lead not only to survival of the observed regimes, but also to better quantitative correspondence between the model and the object. Also, if the observed behavior is general, small variations of connectivity matrix should not lead to disappearance of the desired regime.

The current study aims to show that the spike-wave discharge model in the form of radioengineering circuit (ensemble of electronic oscillators) is well scaled and can reproduce a distribution of seizures by length in population observed experimentally.[4,5]

2. MATHEMATICAL MODEL OF A HIERARCHICAL NEURAL NETWORK

Each individual neuron was built as complete FitzHugh–Nagumo model.[6,7] All couplings were sigmoid:

$$\begin{aligned} \varepsilon \dot{u}_i(t) &= u_i(t) - c_i u_i^3(t) - v_i(t) + \sum_{j \neq i} k_{ij} h\left(u_j(t)\right), \\ \dot{v}_i &= u_i(t) + a_i - b_i v_i(t), \qquad (1) \\ h(u) &= \frac{1 + \tanh(u)}{2}, \qquad (2) \end{aligned}$$

Further author information: (Send correspondence to Nikita M. Egorov)
Nikita M. Egorov: E-mail: egorov.n.m.omnis@gmail.com

Computational Biophysics and Nanobiophotonics, edited by Dmitry E. Postnov, Boris N. Khlebtsov,
Proc. of SPIE Vol. 12194, 1219403 · © 2022 SPIE · 1605-7422 · doi: 10.1117/12.2623993

where u is dimensionless function analogous to the transmembrane potential in biological excitable tissue; v is dimensionless function similar to slow recovery current; t is dimensionless time; ε is inertia parameter; a and b are dimensionless parameters that control the neuron's own dynamics; c is integration constant. The model describes regenerative self-excitation of voltage on the cell membrane (variable u) as a result of nonlinear positive feedback. as well as "recoverv" as a result of linear negative current feedback (variable v).

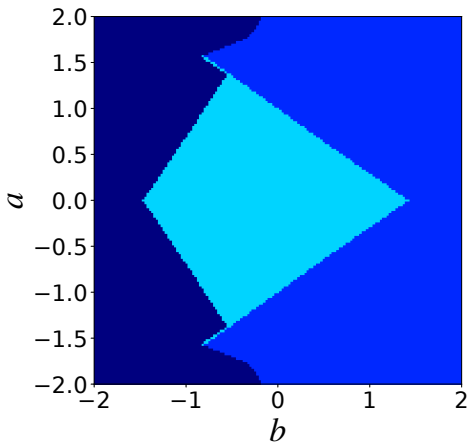

Figure 1. Chart of dynamical regimes for mathematical model of FitzHugh–Nagumo neuron at the parameter plane (a, b). Parameters $\varepsilon = 0.1$ and $c = 1/3$.

The chart of dynamical regimes on the (a, b) plane (section of the parameter space with the hyperplane $\varepsilon = 0.1$, $c = 1/3$) constructed for the individual oscillator was plotted in fig. 1. The chart was plotted using Poincare section of the phase space with the line $u = 0$ using time series of 50 dimensionless time units (seconds) length (500 time points). The parameters a and b were varied in the range $[-2; 2]$ with the step 0.025. Dark blue area corresponds to absence of any attractors, blue area — to stable fixed point and light blue — to the simple limit cycle (period 1 cycle). No other regimes can be found in the singe oscillator.[8]

Synapses are described by the activation function. Often, the sigmoid function is used as an activation function in neural networks. The sigmoid activation function means depolarisation within a neuronal population to expected firing rate. It can be interpreted as a cumulative density function on depolarisation within a population.[9] Hyperbolic tangent function is classically used as a sigmoid function being a particular case of the more general Richard's curve;[10] in our case it was shifted and scaled to match the desired range $[0, 1]$, as it is shown in the formula (2).

In cell biophysics all synapses are divided into excitatory and inhibitory ones. Excitatory (mostly, glutamatergic) synapses facilitate pulse appearance on the postsynaptic membrane, depolarizing it and making the action potential to be possible. In contrary, inhibitory (mostly, GABAergic) synapses prevent or stop generation of action potentials at postsynaptic membrane. In the model (1) the positive values of coupling coefficient k_{ij} correspond to excitatory synapses and negative ones — to inhibitory ones.

Then, two neurons were coupled by sigmoid coupling in the mathematical model. Two connectivity mechanisms were considered: symmetric coupling (both either excitatory or inhibitory) and asymmetric coupling when one neuron excited the other, and the other inhibited the first one. Using Poincare section by the line $u = 0$ in both subsystems, the charts of dynamical regimes were constructed for both oscillators in all considered cases in the same parameter region and with the same step using the series of the same length as previously for a single oscillator. The parameters a, b, k were changed synchronously, assuming that in a real netwoks nearby cells cannot be upset by the parameters significantly.

Charts plotted for two different coupling parameter values are shown in the fig. 2: for $k = 0.1$ in the upper row and for $k = 1.0$ in the lower one. From the left to the right the columns correspond to: symmetric excitatory coupling (neurons were equal, only one is presented), symmetric inhibitory coupling (neurons were equal, only one is presented), asymmetric coupling (excitatory driven neuron) and asymmetric coupling (inhibitory driven neuron). The analysis of the plots indicates that for the for symmetric excitatory coupling (fig. 2 (a,e)) new complex regimes appear near the border between the simple limit cycle and attractorless area, though for the symmetric inhibitory coupling (well visible only in fig. 2 (f) for larger coupling strength) the complex regimes appear between the region of the simple cycle and fixed point area. The asymmetric coupling provides richer regime set and in larger area than both types of the symmetric one, see fig. 2 (c,d,g,h).

We follow the notation used in the papers,[3,11] introducing brief designations for each type of cells involved in the model: cortical interneuron — IN (1 element), cortical pyramidal cells — PY (4 elements), thalamocortical

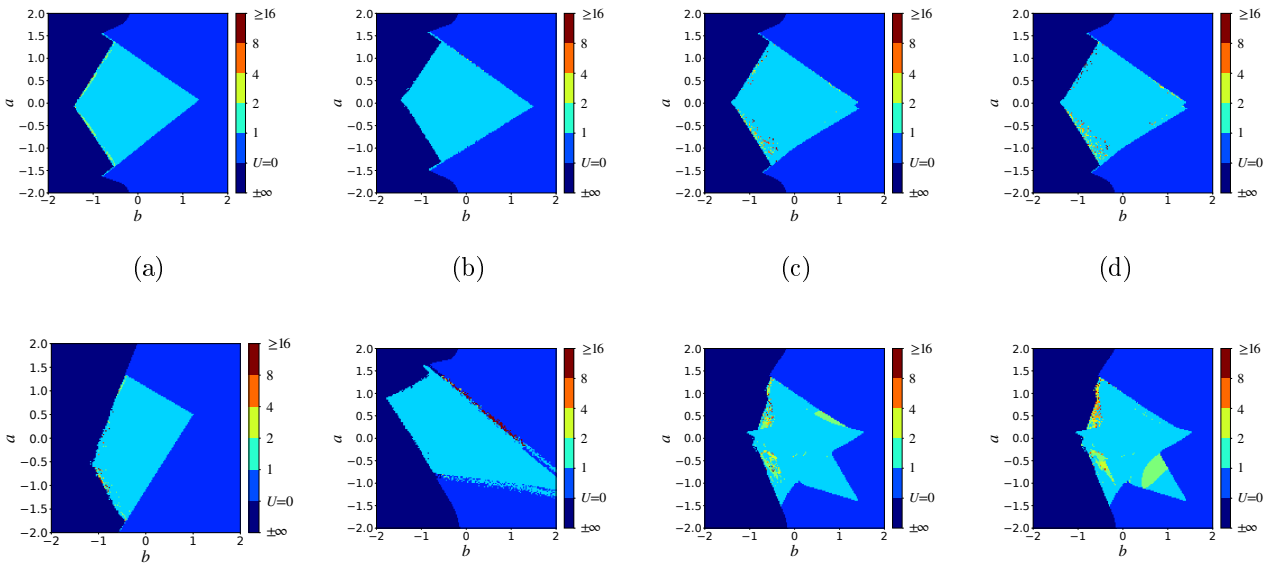

Figure 2. Chart of dynamical regimes for two coupled neurons at the parameter plane (a, b). Parameters $\varepsilon = 0.1$ and $c = 1/3$. (a) symmetric excitatory coupling $k = 0.1$; (b) symmetric inhibitory coupling $k = -0.1$; (c) asymmetric coupling $k = \pm 0.1$ (excitatory driven neuron); (d) asymmetric coupling $k = \pm 0.1$ (inhibitory driven neuron); (e) symmetric excitatory coupling $k = 1.0$; (f) symmetric inhibitory coupling $k = -1.0$; (g) asymmetric coupling $k = \pm 1.0$ (excitatory driven neuron); (h) asymmetric coupling $k = \pm 1.0$ (inhibitory driven neuron).

cells — TC (4 elements), reticular cells of thalamus — RE (4 elements), the external input (nervus trigeminus) neuron — NT (1 element). NT neuron can excite (positive coupling, i. e. $k_{ij} > 0$) one TC cell, TC cells excite all other types of cells except themselves and NT. PY cells can excite cells of all other types except NT, but including cells of the same type. RE cells inhibit (negative coupling, i. e. $k_{ij} < 0$) some cells of all other types except NT, and IN cells can inhibit only PY cells.

Two different absolute values $|k_{ij}|$ were used. One value k_{br} (the subscript corresponds to "brain") was used for all connections inside the model of thalamocortical brain network, and the other one k_{NT} (the subscript corresponds to "nervus trigeminus") was the coupling coefficient from the external input. The mean values of the parameters a and b of the thalamocortical network are $\overline{a}_{br}$ and $\overline{b}_{br}$. The mean values for these parameters for the NT generator were a_{NT} and b_{NT}.

3. ELECTRONIC REALIZATION OF A SINGLE NEURON

A circuit diagram of the constructed complete FitzHugh–Nagumo electronic oscillator is shown in Fig. 3. The circuit contains two analog multipliers U1 and U2 and two dual operational amplifiers U3 and U4. Elements U4B and U3A are integrators, element U4A is a inverter, element U3B is a follower. R_a and R_b are potentiometers that allow you to change the value of parameters a and b. This circuit was constructed in the development of previously constructed reduced electronic oscillator,[12] the another scheme different in detail was also proposed previously.[13]

In contrast to the mathematical model, see Eq. (1), the parameters of the radioengineering circuit have dimensions. The time-scale parameters have the values $E = R_{11}C_1$ and $T = R_7C_2$. Parameter ε from (Eq.1) is calculated as $\varepsilon = E/T$. Parameters $c = (R_3 + R_4)/R_3$ and $b = R_6/(R_5 + R_b \cdot \frac{B}{100\%})$ (B — percentage of potentiometer R_b used) are scaling factors at U and V respectively. Coupling coefficient k is calculated as $k = R_{13}/R_{14}$.

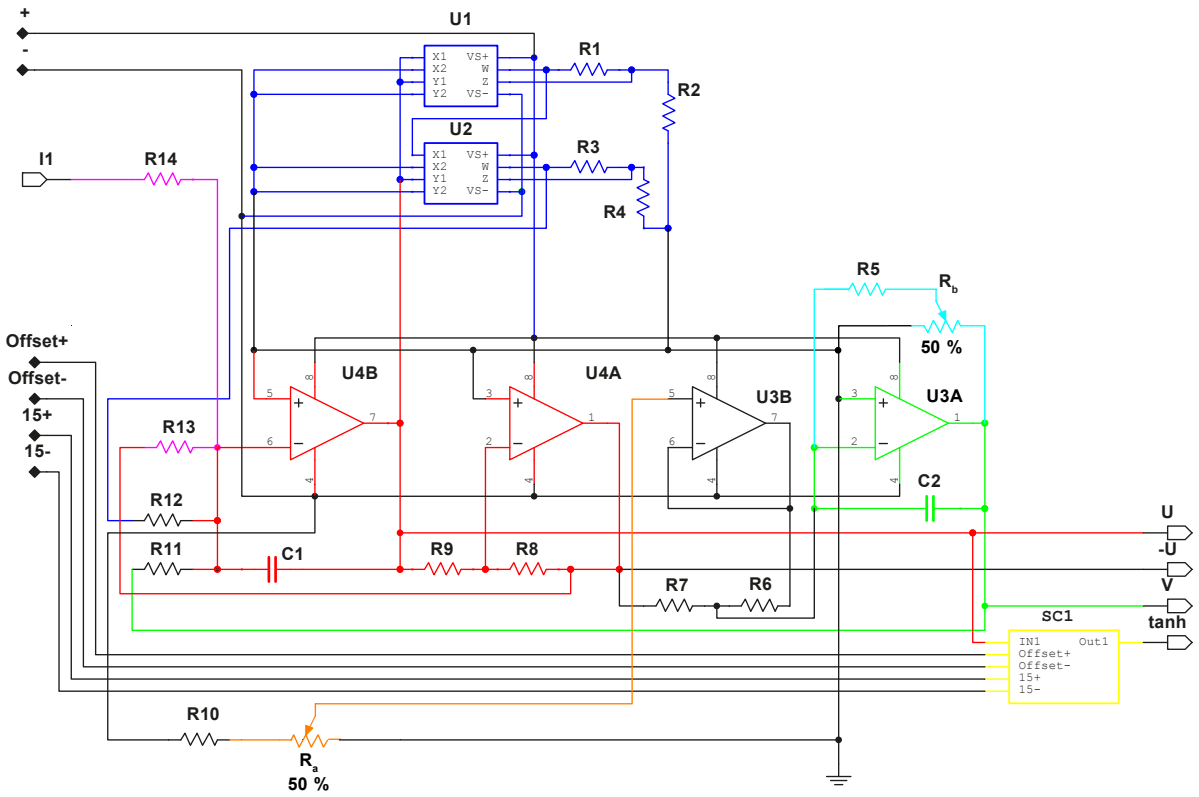

Figure 3. Circuit diagram of a single complete FitzHugh-Nagumo neuron. Red color: u, blue color: cu^3, green color: $-v$, cyan color: b, orange color: a, pink color: k. $R_1 = R_3 = 1$ kΩ, $R_2 = 9$ kΩ, $R_4 = 2.333$ kΩ, $R_a = 1$ kΩ, $R_{10} = 5$ kΩ, $R_b = 4.7$ MΩ, $R_5 = 51$ kΩ, $R_6 = R_7 = R_8 = R_9 = R_{11} = R_{12} = R_{13} = 100$ kΩ, R_{14} depends on coupling strength k, $C_1 = 1$ nF, $C_2 = 0.01$ uF, U1, U2 are amplifiers of the type AD633, and U3, U4 are amplifiers of the type AD822.

The parameter a is set by the voltage at the "+" clamp of the amplifier U3B. The total voltage drop on a series-connected resistor $R10 = 5$ kΩ and potentiometer $R_a = 1$ kΩ is $U_a = 15V$, i. e. the voltage drop on the entire potentiometer is 2.5 V. In particular, if the potentiometer is set to $A = 0\%$, the voltage 2.5 V is set to "+" input of U3B, and if the potentiometer is set to $A = 100\%$, this voltage is zero. So, the parameter a can be calculated using A measured in percents of potentiometer use as follows: $a = 2.5(1 - \frac{A}{100\%})$. It is set in volts as variables u and v actually do in the scheme (let their dimensional values be denoted as U and V).

The cubic transformation is provided by the amplifiers U1 and U2. Integrators U4B and U3A allow to obtain U and V, respectively. Inverter U4A allows to obtain $-U$. Follower U3B is used for connection to the circuit of potentiometer R_{10}. Input $I1$ receive signal from the other neuron.

4. ELECTRONIC REALIZATION OF A SYNAPSE

A circuit diagram of the sigmoid activation function is shown in Fig. 4. The scheme was taken from the work[14] with minor changes. The circuit contains a dual operational amplifier U1 and four bipolar junction transistors Q1–Q4. The inverting amplifier U1A has a gain of 0.05. The differential amplifier U1B has a gain of 0.5. The transistors are connected according to the H-bridge scheme. Difference between excitatory and inhibitory couplings was realized by a switcher, which rearranged chip legs 5 and 6 of the amplifier U1B.

Excitatory coupling was organized as $k \cdot h(u)$, $k > 0$. For positive values of u, if the pulse was generated in the driving neuron, the potential at the driven one was increased up to value equal to k, since $0 \leq h(u) \leq 1$. This could lead to generation of pulse (action potential) at the driven neuron if its one potential plus the driving potential were larger than 0, then, this pulse can spear further along the network. If $u < 0$ for $k > 0$, no significant changes in the dynamics of the driven generator would be caused, since the driving would be zero or

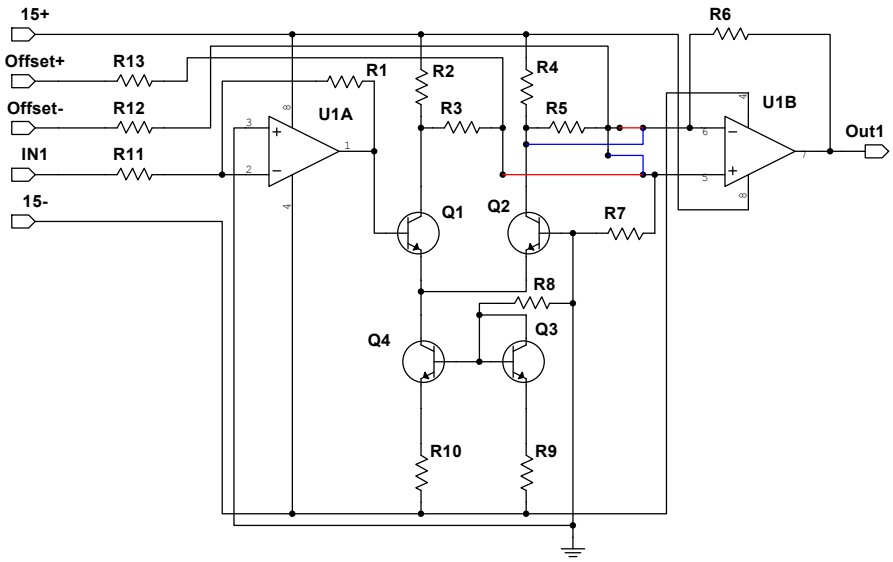

Figure 4. Circuit diagram of the sigmoid activation function in form hyperbolic tangent function. $R1 = 0.52$ kΩ, $R_2 = R_4 = 1$ kΩ, $R_3 = R_5 = R_{11} = R_{12} = R_{13} = 10$ kΩ, $R_6 = R_7 = 5$ kΩ, $R_8 = 9.8$ kΩ, $R_9 = R_{10} = 2$ kΩ, Q1, Q2, Q3, Q4 were bipolar junction transistors 2N1711, U1 was an amplifier of the type NE5532AI. Red color: excitatory coupling; blue color: inhibitory coupling.

close to zero for $u \lessapprox 0$. If $u \lessapprox 0$ some subthreshold oscillations can appear in the driven neuron, but they do not have any significant biological meaning and cannot spread further.

The inhibitory coupling was organized in the same manner as excitatory one, but with $k < 0$. The pulse from the driving neuron comes to the driven one and suppresses its activity. If the driven generator was generating it can stop since it summary potential becomes less then 0, with its pulses no longer spreading across the network. If the driven neuron was not generating, inhibitory pulse leads to additional overinhibition, which will be compensated with time by itself, since the cell tends to keep the constant resting state potential about 400–70 mV. normally, the same neurons achieve both excitatory and inhibitory inputs and the resulting activity depends on their amount and synchrony.

To test the electrical synapse (fig. 4) for correctness of work, a harmonic signal of 2 V amplitude was introduced as a driving. the resulting postsynaptic signal was compared to the mathematical model, see Fig. 5. In the mathematical model the driving signal was put into the activation function (2) with $k = \pm 1$, providing excitatory and inhibitory couplings respectively. In the circuit inhibitory and excitatory couplings were organized by a switch. The simulation of the electronic circuit well matches the results of mathematical modeling as it can be seen from the Fig. 4.

5. ELECTRONIC REALIZATION OF THREE COUPLED NEURONS

Then, we tested the scheme of three unidirectionally coupled neurons. The first neuron N1 was in oscillatory mode ($\varepsilon_{N1} = 0.1$, $a_{N1} = 0.8$, $b_{N1} = 0.2$, $c_{N1} = 1/3$), the second neuron N2 and the third one N3 were in excitable mode (no self-oscillations, $\varepsilon_{N2} = \varepsilon_{N3} = 0.1$, $a_{N2} = a_{N3} = 0.6875$, $b_{N2} = b_{N3} = 0.8$, $c_{N2} = c_{N3} = 1/3$). Coupling from N1 to N2 was always excitatory with coupling coefficient $k = 0.2$. The coupling from N2 to N3 was either excitatory or inhibitory.

The Fig. 6 shows the correctness of the proposed scheme: the excitatory couplings can spread along the network, inducing oscillations in the passive neurons which were out of self-oscillatory activity, while inhibitory coupling does not lead to any oscillations in such neurons and only can cause low level under-threshold activity.

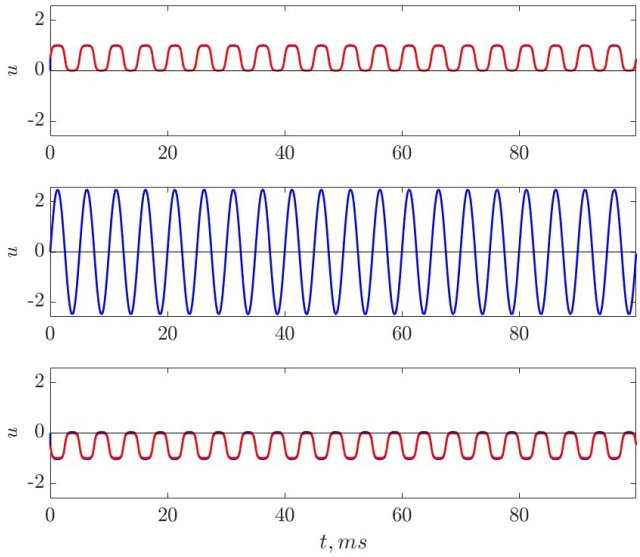

Figure 5. Time series of mathematical model (red lines) and electrical circuit (SPICE simulation, blue lines). From top to bottom: excitatory coupling after a synapse, driving signal, inhibitory coupling after a synapse.

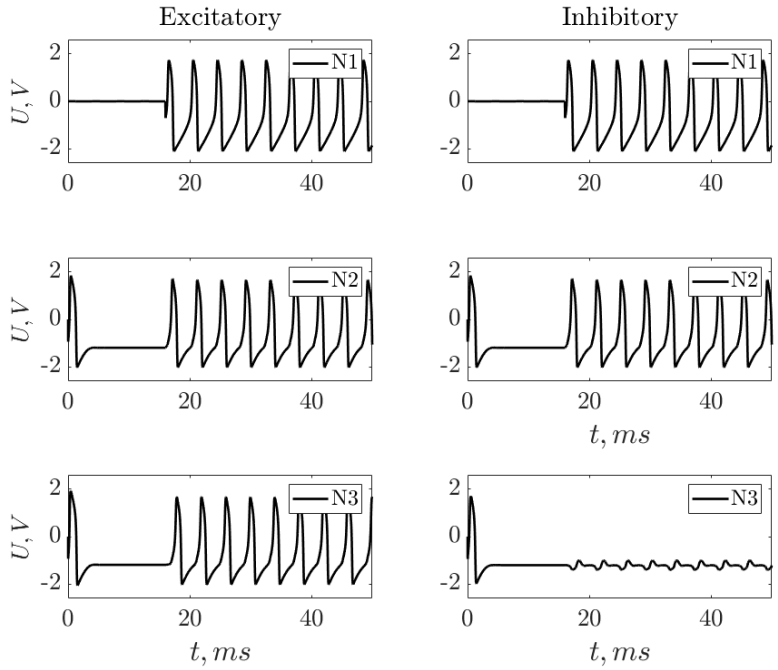

(a) (b)

Figure 6. Time series for three unidirectionally coupled neurons: N1 → N2 → N3. The neuron N1 always was in the oscillatory regime, neurons N2 and N3 were the under-threshold excitable mode. The coupling from N1 to N2 was always excitatory. The coupling from N2 to N3 could be excitatory (a) or inhibitory (b).

6. CIRCUIT DIAGRAM OF HIERARCHICAL NEURAL NETWORK

The electronic circuit for modeling absence epilepsy was developed previously in[1] using electronic generators, corresponding to incomplete FitzHugh–Nagumo neurons[12] with linear coupling as it was proposed previously.

But realistic excitatory/inhibitory coupling could not be organized using these simplified models due to both positive and negative coupling led to initiation of oscillatory activity in the passive under-threshold generators. To overcome this disadvantage we used the scheme of the generator and the synapse proposed here. The entire circuit was constructed from 14 generators, one of which was in self-generating mode with and was considered as external input to thalamocortical system from peripheral, as it was proposed for absence epilepsy in experimental research[2] and in models.[15] Further, we denote it as NT (nervus trigeminus). All other generators were equal by parameters as much as it is possible in practice and were denoted as "br" neurons (from "brain"). The brain neurons were split into 4 clusters: modeling cortical pyramids (4 generators), modeling cortical interneuron (1 generator), modeling thalamocoatical cells (4 generators) and modeling reticular cells (4 generators). The connectivity matrix was taken from the previous work.[1]

When an epileptic seizure is initiated, a relatively short train of pulses arrives from NT to the thalamus to induce oscillations in the network. In the circuit, the seizure is initiated by short-time (20 ms, 5 periods of the external signal) opening of switch SI after 17 ms of simulation (Fig. 7). The open switch transmits the signal of external neuron NT to the network. First, we observe the induced oscillations that are retained during a certain time interval after termination of the pulse. The time series show the absence of oscillations in an interval from the termination of the primary transient process corresponding to the switching-on of the setup to the moment at which the external signal was fed to the system. After termination of the external signal, the system exhibits oscillations (about four periods). In a time interval of 20 ms after the moment at which the external signal was fed to the system, all neurons of the network were involved in oscillations (transient process corresponding to the development of the induced oscillations), so that we observe an irregular low-amplitude signal.

The curves in Fig. 7 were plotted for the following parameters: $\varepsilon_{NT} = \varepsilon_{br} = 0.1$, $a_{NT} = 0.425$, $a_{br} = 0.98$, $b_{NT} = 0.8$, $b_{br} = 0.08$, $c_{NT} = c_{br} = 1/3$, $k_{NT} = 0.2$, $k_{br} = 0.1$.

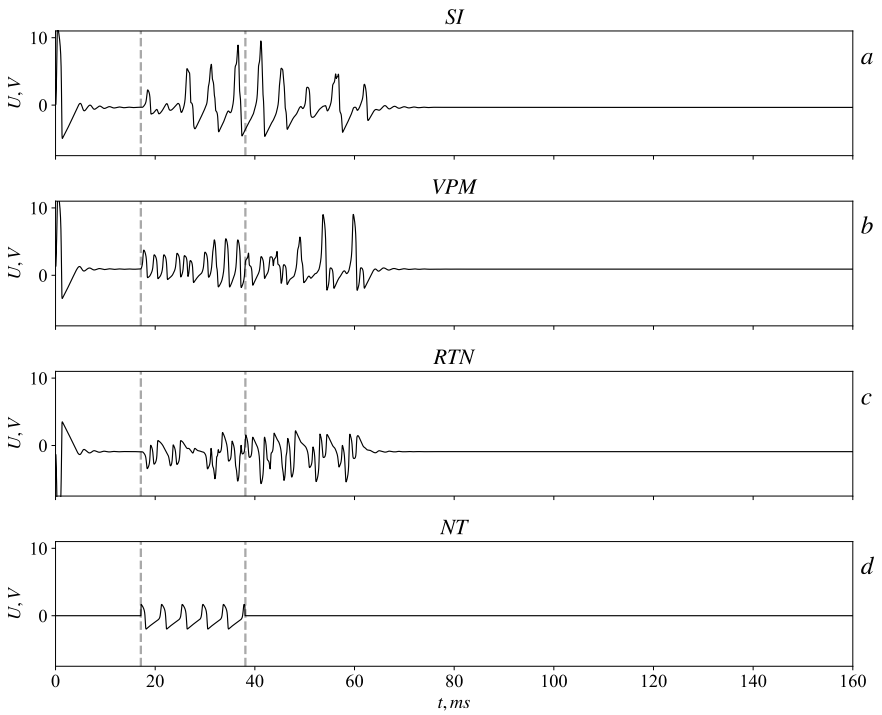

(a) (b)

Figure 7. Time series for integral signals: (a) the primary somatosensory cortex (SI), which includes PY and IN cells; (b) the reticular thalamic nucleus (RTN), consisting of RE-cells; (c) the ventral posteromedial thalamic nucleus (VPM), consisting of TC-cells; (d) the trigeminal neuron (NT). The black lines indicate the beginning and the end of the external driving.

This simulation shows possibility of oscillatory transient processes in the scheme in response to a short pulse activation for the newly developed schemes of generator and synapse, proving the ground principles assumed when constructing model of absence seizures.

7. ACKNOWLEDGEMENTS

This work was supported by Russian Science Foundation, grant No 21-72-00015, https://rscf.ru/project/21-72-00015/.

REFERENCES

[1] N. M. Egorov, V. I. Ponomarenko, I. V. Sysoev, and M. V. Sysoeva, "Simulation of epileptiform activity using network of neuron-like radio technical oscillators," *Technical Physics* **66**(3), pp. 505–514, 2021.

[2] K. R. Abbasova, S. A. Chepurnov, N. E. Chepurnova, and G. Van Luijtelaar, "The role of perioral afferentation in the occurrenceof spike-wave discharges in the wag/rij modelof absence epilepsy," *Brain research* **1366**, pp. 257–262, 2010.

[3] A. A. Kapustnikov, M. V. Sysoeva, and I. V. Sysoev, "Modeling Spike-Wave Discharges in the Brain with Small Neurooscillator Networks," *Mathematical Biology and Bioinformatics* **16**, pp. 139–146, 2020.

[4] C. M. van Rijn, S. Gaetani, I. Santolini, A. Badura, A. Gabova, J. Fu, M. Watanabe, V. Cuomo, G. van Luijtelaar, F. Nicoletti, and R. T. Ngomba, "WAG/Rij rats show a reduced expression of CB1 receptors in thalamic nuclei and respond to the CB1 receptor agonist, R(+)WIN55,212-2, with a reduced incidence of spike-wave discharges," *Epilepsia* **51**(8), pp. 1511–1521, 2010.

[5] L. B. Kalimullina, A. M. Musina, and G. D. Kuznetsova, "Experimental approaches to studies of the role of the genotype at the tag 1a locus of the dopamine d2 receptor in epileptogenesis," *Neuroscience and Behavioral Physiology* **43**(8), pp. 935–940, 2013.

[6] R. FitzHugh, "Impulses and physiological states in theoretical models of nerve membrane," *Biophysical Journal* **1**, pp. 445–466, 1961.

[7] J. Nagumo, S. Arimoto, and S. Yoshizawa, "An active pulse transmission line simulating nerve axon," *Proceedings of the IRE* **50**, pp. 2061–2070, 1962.

[8] A. S. Dmitrichev, D. V. Kasatkin, V. V. Klinshov, S. Y. Kirillov, O. V. Maslennikov, D. S. Shchapin, and V. I. Nekorkin, "Nonlinear dynamical models of neurons: Review," *Izvestiya VUZ. Applied Nonlinear Dynamics* **26**(4), pp. 5–58, 2018.

[9] A. Marreiros, J. Daunizeau, S. Kiebel, and K. Friston, "Population dynamics: Variance and the sigmoid activation function," *NeuroImage* **42**(1), pp. 147–157, 2008.

[10] F. J. Richards, "A flexible growth function for empirical use," *Journal of Experimental Botany* **10**(2), p. 290–300, 1959.

[11] T. M. Medvedeva, M. V. Sysoeva, A. Lüttjohann, G. van Luijtelaar, and I. V. Sysoev, "Dynamical mesoscale model of absence seizures in genetic models," *PLoS ONE* **15**(9), p. e239125, 2020.

[12] D. Kulminskiy, V. Ponomarenko, M. Prokhorov, and A. Hramov, "Synchronization in ensembles of delay-coupled nonidentical neuronlike oscillators," *Nonlinear Dynamics* **98**(1), pp. 735–748, 2019.

[13] S. Binczak, S. Jacquir, J.-M. Bilbault, V. B. Kazantsev, and V. I. Nekorkin, "Experimental study of electrical fitzhugh–nagumo neurons with modified excitability," *Neural Networks* **19**(5), pp. 684–693, 2006.

[14] H. Li, Y. Yang, W. Li, S. He, and C. Li, "Extremely rich dynamics in a memristor-based chaotic system," *The European Physical Journal Plus* **135**, p. 579, 2020.

[15] P. Suffczynski, S. Kalitzin, and F. L. D. Silva, "Dynamics of non-convulsive epileptic phenomena modeled by a bistable neuronal network," *Neuroscience* **126**(2), pp. 467–484, 2004.